

# Chitin Derivatives. I. Kinetics of the Heat-Induced Conversion of Chitosan to Chitin

ACKAH TOFFEY, GAMINI SAMARANAYAKE, CHARLES E. FRAZIER, and WOLFGANG G. GLASSER\*

Biobased Materials Center, and Department of Wood Science & Forest Products, Virginia Polytechnic Institute and State University, Blacksburg, Virginia 24061-0323

## SYNOPSIS

The water-soluble solids comprised of the ionic complex between chitosan and acetic acid, chitosonium acetate, are converted into chitin by heating. The thermally-induced conversion of a water-soluble chitosonium acetate in film form into a water-insoluble chitin film was examined by thermal analysis (DMTA, TGA, DSC, and TMA) and by solid state  $^{13}\text{C}$ -NMR spectroscopy. Results indicate that  $\tan \delta$ -transitions occur at increasingly high temperatures, and over progressively wider temperature ranges, as the transformation progresses. Likewise, the storage modulus,  $\log E'$ , increases as the chitosonium acetate film undergoes "cure" and converts to chitin. Cure kinetic parameters are obtained using the model proposed by Provder et al. modified for glass transition temperature ( $T_g$ ). The results suggest the existence of two sequential first order reactions, an initial and a late cure reaction, having activation energies of approximately 15 and 21 kcal/mol, respectively. © 1996 John Wiley & Sons, Inc.

## INTRODUCTION

Chitin is the principal structural polymer of the exoskeleton of crustaceae as well as of insects.<sup>1</sup> It serves nature as a mechanically strong barrier polymer with significant oxygen diffusivity.<sup>1</sup> Chitin is well recognized by polymer chemists as an attractive linear poly(anhydro *N*-acetyl glucose amine).<sup>2-4</sup> Unfortunately, chitin is notoriously insoluble in all common organic solvents with the exception of dimethyl acetamide (DMAc)/LiCl.<sup>5</sup> Because of its insolubility, chitin is usually converted to chitosan by alkaline hydrolysis. Chitosan, the deacetylated poly(glucose amine), is readily soluble in dilute acetic acid, from which it is usually regenerated by treatment with alkali. The water-soluble ionic complex of chitosan and acetic acid, chitosonium acetate, can be handled like any other soluble linear polymer. It can be cast into films,<sup>6-8</sup> spun into fibers,<sup>9</sup> precipitated into particles from suitable nonsolvents, which revert the ionized ammonium groups back into amine functionality, and crosslinked to produce chitosan fibers.<sup>10</sup> In addition, chitosan blends with

cellulose have been advocated as biodegradable films.<sup>11,12</sup> However, the integrity of chitosan films or fibers is more easily compromised than chitin, because chitosan remains soluble and more susceptible to moisture attack. Thus, a procedure that converts chitosan to chitin holds great promise for the industrial utilization of this abundant biobased material.

The objectives of this article are to present evidence in support of the conversion of the ionic complex of chitosan, chitosonium acetate, to chitin by heating, and to describe the kinetic parameters underlying the conversion. This regeneration of chitin, the restoration of insolubility, and the recreation of characteristics usually found in thermosetting network polymers, can be likened to the process of cure.

## MATERIALS AND METHODS

### Materials

The chitosan used in the preparation of chitosonium acetate was obtained from Sigma Chemicals, St. Louis, MO. This chitosan was obtained by deacetylation of chitin from crab shells, and it had a degree of deacetylation of 89.3% (manufacturer's speci-

\* To whom correspondence should be addressed.

cation). Glacial acetic acid obtained from Aldrich Chemicals, Milwaukee, WI, was used as the solvent for chitosan.

## Methods

### *Chitosonium Acetate Film Preparation*

The preparation of chitosonium acetate films involved a two-stage process. In the first stage, about 100 g of chitosan was dissolved in 7 L of 10% aqueous acetic acid and stirred for about 24 h to obtain a clear, highly viscous solution. This solution was cast into films in large rubber trays from which solvent evaporated. The dried films were then pulverized to obtain powderous chitosonium acetate. In the second stage, 9.5 g of powderous chitosonium acetate were dissolved in 400 mL of water with stirring until a clear solution was obtained. This was cast as films in flat Petri dishes followed by solvent evaporation and drying at room temperature for 2 weeks. Films were produced, the thickness of which ranged from 0.5 to 1.2 mm. Attempts to use vacuum drying resulted in warped films. Samples for thermomechanical analysis were preheated in an oven at temperatures of 80, 100, 120, 130, and 140°C for periods ranging from 5 min to 48 h.

### Differential Scanning Calorimetry (DSC)

A DSC from Perkin–Elmer, model DSC 4, connected to a temperature controller and interfaced to a thermal analysis data station (TADS), was used to assess whether or not the dried chitosonium acetate films contained residual moisture. A freshly cast or well-dried film was sealed in an aluminium pan and heated at a rate of 10°C/min. All experiments were done under a purge of dry nitrogen.

### Dynamic Mechanical Thermal Analysis (DMTA)

Dynamic mechanical thermal analysis of chitosonium acetate films was performed with a Polymer Laboratory DMTA. Samples were tested by bending in a single cantilever mode, at a heating rate of 2.5°C/min, an oscillation amplitude of 0.4 mm, and a frequency of 1 Hz. Typical sample dimensions were 8 × 5 × 1.1 mm. A nitrogen purge at a rate of 25 cm<sup>3</sup>/min was used during data collection. The glass transition temperature was taken as the maximum in the tan  $\delta$  curve.

### Thermomechanical Analysis (TMA)

A TMA from Perkin–Elmer, model TMS-325, was used to determine the glass transition temperature ( $T_g$ ) of heat-treated samples. All experiments were done using the thermal expansion probe and a loading weight of 5 g. The samples were 0.65 mm thick. TMA experiments involved two stages. The first stage addressed the determination of  $T_g$  of the partially cured material, where the material is scanned to a temperature well above the glass transition. This treatment gave a fully cured or converted material (supported by DMTA). The second stage involved scanning of the fully cured material to determine the ultimate  $T_g$  associated with each isothermal temperature.

### Thermogravimetric Analysis (TGA)

A Perkin–Elmer TGA-2 was used to assess the weight loss with heat treatment. All samples were in powderous form, and were heat treated under a purge of dry nitrogen. Heat treatment involved dynamic (at a heating rate of 5°C/min) and isothermal mode (at 110°C for 6 h).

### CP/MAS NMR Spectroscopy

Solid-state NMR experiments were carried out on a Bruker MSL-300 at a resonance frequency of 75.47 MHz for <sup>13</sup>C nuclei. The proton spin-lock field strength was approximately 56 KHz. Powderous chitosonium acetate, untreated and heat treated, were loaded into a zirconium oxide rotor. The magic angle was set using the KBr method, and the rotor was spun at 5 KHz. The Hartmann–Hahn match was established with adamantane. Standard phase cycling was used to obtain the spectra. Cross-polarization contact time was 1 ms. A delay time of 3.75 s was used between successive pulses, and 1000 scans were accumulated for each experiment. Signal assignments were based on literature values.

## RESULTS AND DISCUSSION

### Thermal Analysis

The process of cure has been described by Gillham<sup>13</sup> in terms of the so-called time–temperature transformation (TTT) diagram (Fig. 1). The TTT diagram provides an illustration of the morphological changes a thermosetting network polymer undergoes in response to time at isothermal cure temperature. The process commences with “gelation,” the for-

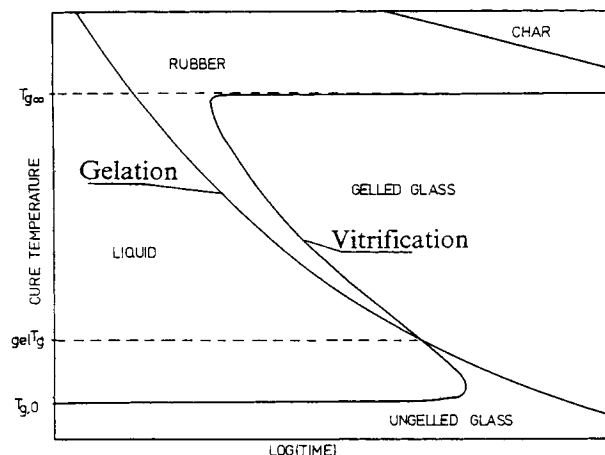


**Figure 1** The time-temperature-transformation (TTT) cure diagram of Gillham<sup>13</sup> showing the various events and states associated with cure of a thermoset.

mation of an infinite polymer network. Gelation precedes vitrification, which is described as the moment when the rising glass transition temperature of the network undergoing cure reaches the isothermal cure temperature. Gelation and vitrification are two events in a cure process that convert a low modulus liquid into a high modulus infinite network. Transitions of the damping behavior,  $\tan \delta$  or loss modulus,  $\log E''$ , of the DMTA spectrum can be used to analyze the cure process.<sup>14</sup> Typical DMTA spectra of an amine-cured epoxy at two isothermal cure temperatures are shown (Fig. 2).<sup>14</sup> Two distinctive transitions associated with gelation and vitrification are observed. At the onset of cure, the liquid-state resin exhibits low damping. Damping increases as the resin becomes rubbery, and it declines again after gelation due to restrictions on chain mobility. Damping exhibits a second maximum as the rubbery material transforms to the glassy state, in a similar fashion as the glass to rubber transition. Thus, gelation and vitrification are thermal events that give rise to distinctive transitions by dynamic mechanical thermal analysis (Fig. 2).<sup>14</sup> Both gelation and vitrification occur after a short time exposure at the higher temperature. This observation is always true of the time to gelation; however, the time to vitrification is dependent on the relative values of the isothermal cure temperature and the ultimate  $T_g$  of the fully cured polymer. When a moisture-free chitosonium acetate film is exposed to isothermal cure conditions in a dynamic mechanical thermal analysis (DMTA) instrument, changes in  $\tan \delta$  and  $\log E'$  are recorded (Fig. 3). The  $\tan \delta$ -transitions occur after shorter time periods when heated at 140°C as compared to 100°C; and the storage modulus rises

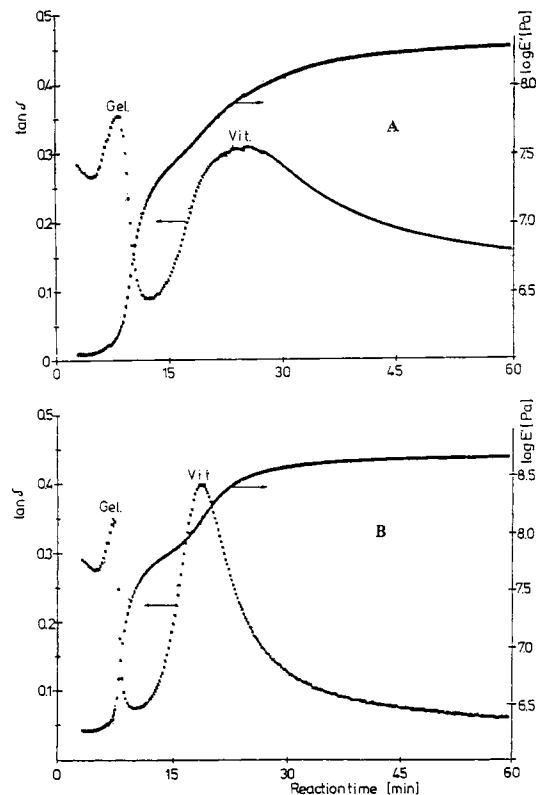


**Figure 2** Isothermal cure profiles of an amine-cured epoxy resin at two temperatures (A: 130°C, B: 140°C). The  $\tan \delta$  curves give distinct transitions identified with gelation and vitrification. The times to both gelation and vitrification were shorter at the higher temperature.

more rapidly at the higher temperature. Both transitions reveal a distinctive separation into two sub-events, which overlap each other and which form a

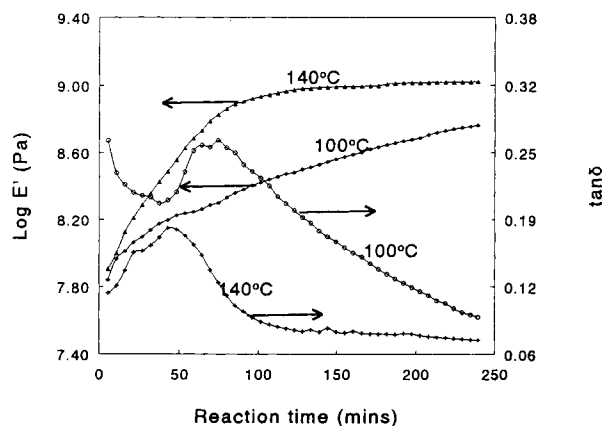


**Figure 3** Isothermal cure profiles of chitosonium acetate (ChAc) at two temperatures, 100°C and 140°C. The storage modulus shows a progressive increase with time, and the  $\tan \delta$  shows two overlapping transitions.

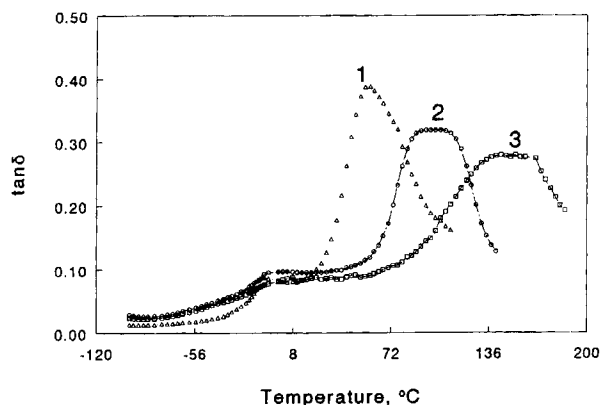


**Figure 4** DMTA spectra of chitosonium acetate subjected to sequential heat treatments. There is a progression of  $T_g$  to higher value with each scan, and a corresponding decline in peak height. 1, 2, and 3 represent first, second, and third scans, respectively.

broad overall transition (Fig. 3). Whereas it is difficult to ascribe these transitions and/or modulus increases to either gelation or vitrification as in thermosets, it is apparent that there is a heat-induced transformation of the material that takes a two-step process. The pattern of the DMTA spectrum is typical of the cure behavior of a thermoset (Fig. 2).

When a chitosonium acetate film is scanned by DMTA from a temperature of  $-110^\circ\text{C}$  to various

elevated temperature levels,  $\tan \delta$ -transitions are observed that are located at progressively higher temperatures in addition to being progressively smaller in height and broader in width (Fig. 4). This indicates a shift of  $T_g$  to higher temperatures as the temperature range over which the sample is scanned increases. This phenomenon is consistent with the cure behavior of thermosets. A similar pattern is observed during sequential heat treatments of chitosan films.<sup>15</sup> The rising glass transition temperature is attributed to the removal of residual moisture, which plasticizes the material. In the case of chitosonium acetate, loss of residual moisture is evidently not responsible for the rising glass transition temperature. DSC studies suggest loss of residual moisture from a freshly-cast chitosonium acetate film. This is evident in a DSC thermogram, where there is a well-resolved endotherm at  $100^\circ\text{C}$  due to evaporation of residual moisture (Fig. 5). A similar, but well-dried material did not indicate any trace of residual moisture. This is supported by the absence of an endotherm at  $100^\circ\text{C}$  (Fig. 5).

Likewise, chitosonium acetate films preheated for 4 h, each, at different temperature levels, reveal  $\tan \delta$ -transitions that occur at progressively higher temperatures and that diminish in size and slightly broaden in width (Fig. 6). A similar trend of declining peak height is observed for samples heated at a constant isothermal temperature of  $110^\circ\text{C}$  for

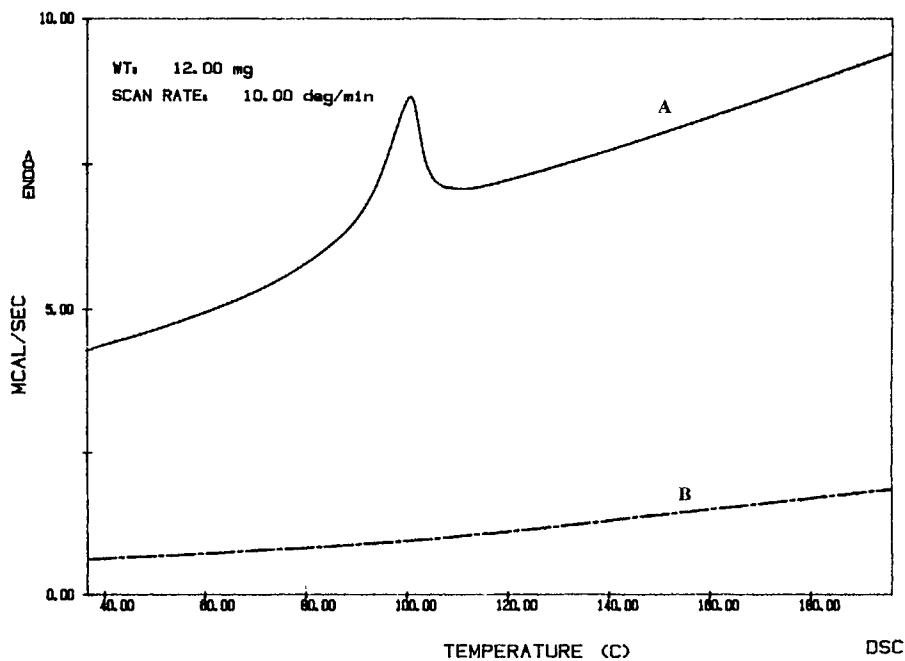


**Figure 5** A differential scanning thermogram of freshly cast (A), and dried (B) chitosonium acetate films. A well-resolved endotherm due to the loss of residual moisture is apparent at  $100^\circ\text{C}$  for A.

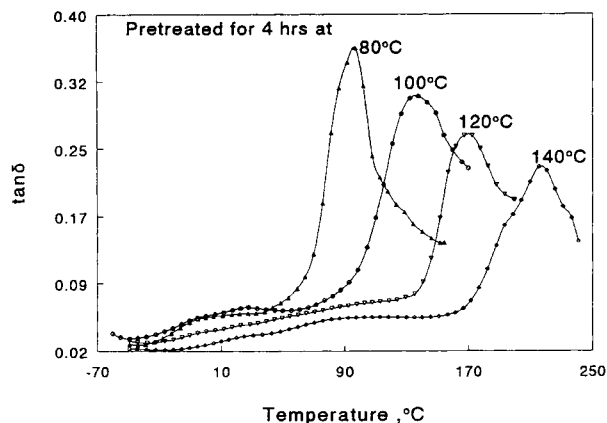


**Figure 6** Dynamic scan of chitosonium acetate heat treated at various temperatures for 4 h. As the temperature is raised, there is a progression of  $T_g$  to higher values, and a decline of the peak height of the transition. This is a behavior that parallels that of a thermoset at different crosslink densities.

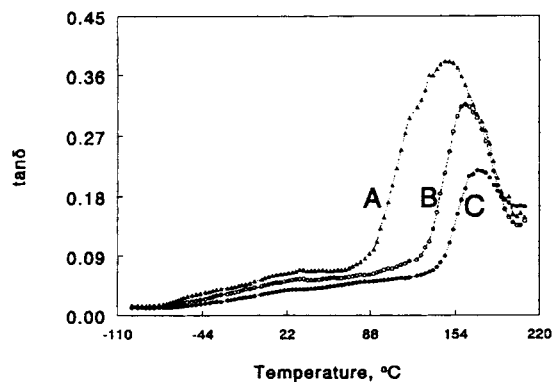
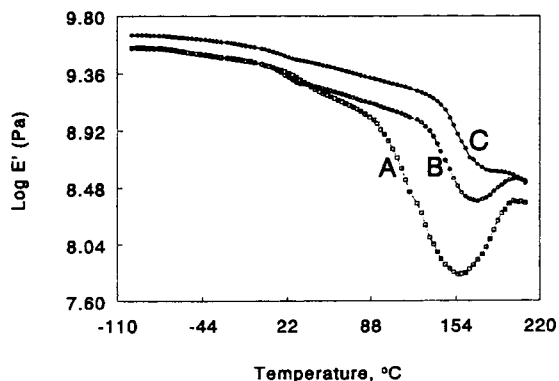


**Figure 7** Top: storage modulus profile of chitosonium acetate heat treated at 110°C for various periods. Bottom: damping profile of the same material. A, B, and C represent 2 h, 4 h, and 12 h of heat treatment at 110°C, respectively.

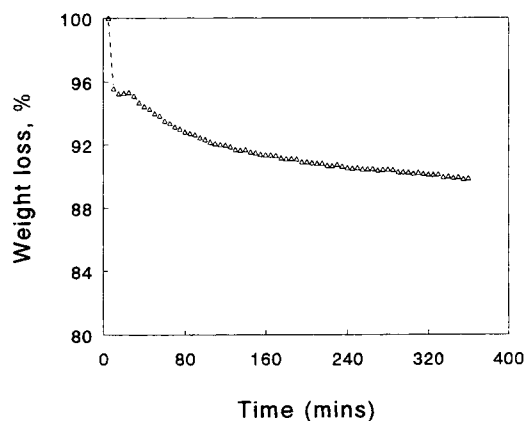
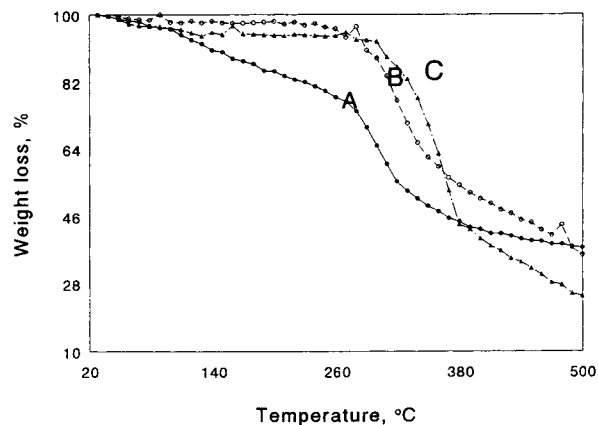


**Figure 8** (a) Relative stability of chitosonium acetate (A), heat-treated chitosonium acetate (B), and native chitin (C). The degradation profile of heat-treated chitosonium acetate mirrors that of native chitin, and supports the assertion that there is a thermally triggered conversion of chitosonium acetate to chitin (top). (b) Thermogravimetric analysis spectrum of powderous chitosonium acetate at an isothermal temperature of 110°C. The loss of weight never attains an equilibrium; but, it is approximately equivalent to the theoretical weight loss expected in the conversion of chitosonium acetate to chitin (bottom).

varying periods. In this case, the rise in glass transition temperature is paralleled by an increase in storage modulus after the glass-to-rubber transition region, and this suggests further transformation of a partially transformed material (Fig. 7). A similar trend has been observed with an amine-cured epoxy.<sup>14</sup> This supports the assertion that the thermally-induced transformation of chitosonium acetate can be likened to the cure reaction of a thermoset.

When powderous chitosonium acetate is exposed to heating by thermogravimetric analysis (TGA), a progressive loss of mass is recorded even below ca. 250°, the temperature at which chitin and chitosan begin to thermally degrade [Fig. 8(a)]. Isothermal

heating at 110°C results in a gradual loss of mass over prolonged periods of time without ever reaching an equilibrium level. However, mass loss approaches 9% after 6 h, a value comparable to the theoretical loss of mass for the conversion of chitosonium acetate to chitin, i.e., 8.1% [Fig. 8(b)].

### NMR Spectroscopy

The analysis of chitin, chitosan, and chitosonium acetate following different levels of heat treatment (Figs. 9–14) reveals signals representing, among others, acetyl functionality. The N-acetyl group of chitin raises signals at 23 ppm (CH<sub>3</sub> group), and at 173 ppm (N-acetyl CO functionality) (Fig. 9). Following deacetylation, both peaks disappear from the <sup>13</sup>C-NMR spectrum (Fig. 10). Chitosonium acetate raises signals at 23 ppm (CH<sub>3</sub> group), and at 179 ppm (acetate-CO carbon) (Fig. 11).

Solid chitosonium acetate partially preheated raises signals at 23 ppm, at 173 ppm, and at 179 ppm (Fig. 12). When this partially “cured” chitosonium acetate film is treated with mild, cold alkali so as to neutralize ionically bound acetate groups, the remaining solids display a CO-carbon signal at 173 ppm (Fig. 13). The transition the CO-carbon signals

undergo in response to severity of heat treatment are illustrated (Fig. 14). The signal at 179 ppm representing CO-acetate functionality gradually reverts to a signal centered at 173 ppm representing N-acetyl CO functionality. Intermediate levels of conversion represent two distinct peaks, which change in proportion in relation to heat treatment. These changes point to chitosonium acetate to chitin transformation.

Using acetic acid solutions of chitosan and finely suspended cellulose powder, Hosokawa et al. formed strong composites by heating.<sup>11</sup> Carbonyl enrichment of the cellulose component of such composites by oxidation with ozone was reported to result in strength improvements. The conclusion of this study was that the strength increase supposedly was due to crosslinking of chitosan with the carbonyl groups of cellulose. However, when similar experiments were repeated by the same authors with acids other than acetic acid, no strength increase was observed.<sup>11</sup> If the strength improvements were due to crosslinking, similar observations should have been made with acids other than acetic acid. This is because other acids would not hinder crosslinking. An alternate explanation is that there was a thermally triggered transformation of the ionic complex of

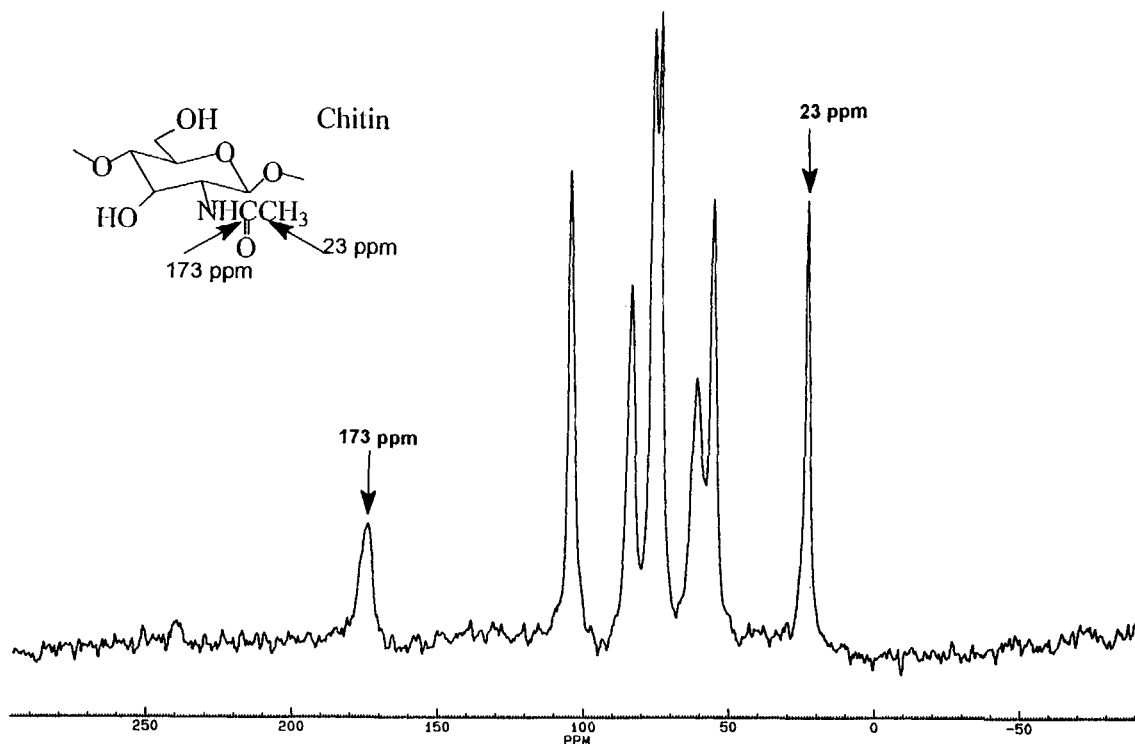


**Figure 9** CP-MAS <sup>13</sup>C-NMR spectrum of chitin. The peaks at 23 and 173 ppm are identifiable as methyl (CH<sub>3</sub>) and N-acetyl carbonyl groups, respectively.

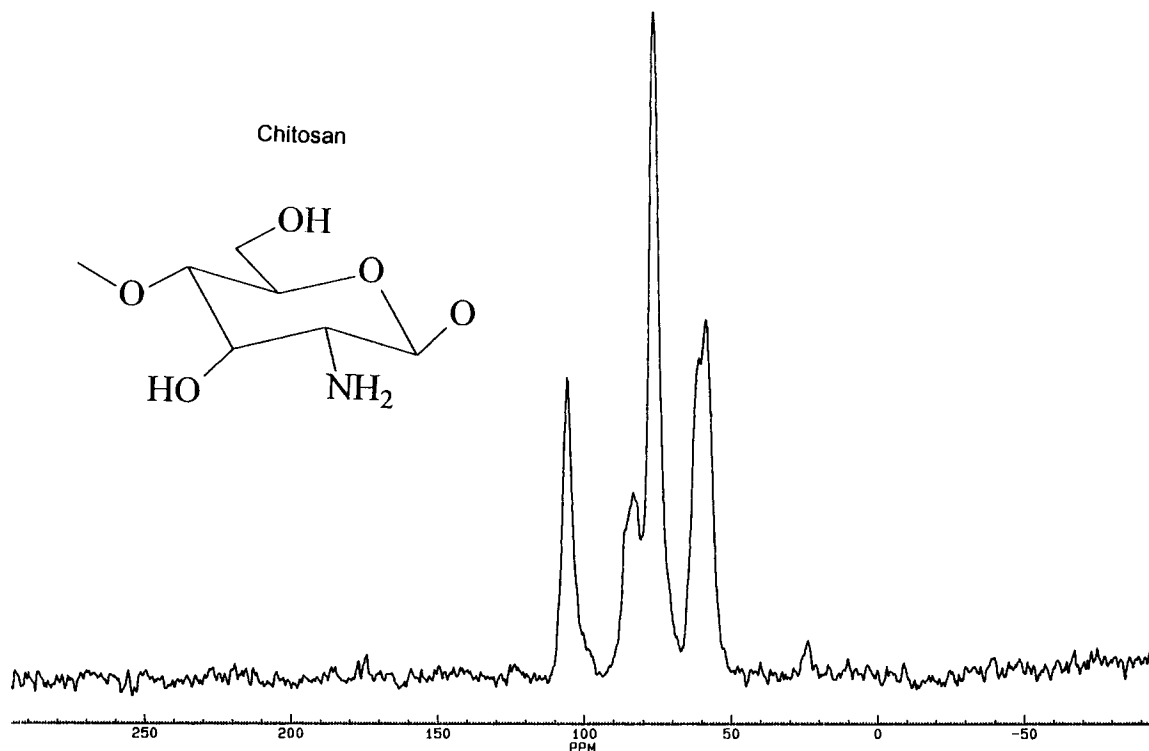


**Figure 10** CP-MAS  $^{13}\text{C}$ -NMR spectrum of chitosan. Both the methyl and *N*-acetyl carbonyl peaks disappear due to deacetylation.

chitosan to chitin, which was manifested in an improvement of strength.

### Kinetic Considerations

The process of cure has been kinetically described by Provder et al. in terms of modulus change.<sup>16</sup> Extent of cure,  $F$ , was reported to be a function of modulus,  $G$ , for samples having been cured at time  $t$  and temperature  $T$ ,

$$F_{(t,T)} = G_{(t,T)} - G_{(0)} / G_{(\infty)} - G_{(0)} \quad (1)$$

where  $G_{(0)}$ ,  $G_{(t,T)}$ ,  $G_{(\infty)}$  are the modulus at the onset of cure, the modulus at a given time, and the ultimate modulus of the material, respectively. Using this definition of extent of cure, a kinetic rate constant describing a first order cure process is derived from

$$-\ln(1 - F) = k_{(T)} t \quad (2)$$

where  $t$  represents time and  $k$  represents rate constant. Using this first order rate equation, and adapting it to the more sensitive changes in  $T_g$  as opposed to modulus, a modified form of the model of Provder et al. can be formulated

$$F_{(t,T)} = T_{g(t,T)} - T_{g(0)} / T_{g(\infty)} - T_{g(0)} \quad (3)$$

where  $T_{g(0)}$ ,  $T_{g(t,T)}$ , and  $T_{g(\infty)}$  are the glass transition temperature at the onset of cure, at a given time under isothermal cure, and at full cure, respectively.

The first order rate equation [eq. (2)] can be expressed in Arrhenius form,

$$\ln k_{(T)} = \ln A - E/RT \quad (4)$$

from which the activation energy,  $E$ , for a reaction can be derived in the usual manner.

Changes in glass transition temperature, determined by TMA, over time for isothermal cure experiments conducted at different temperatures (Fig. 15) show a progressive rise with cure temperature, similar to the behavior of thermosets. The ultimate  $T_g$  of fully cured chitosonium acetate was taken as the average of values determined for the various isothermal temperatures, and this was determined to be 189°C. The  $T_g$  of unheated chitosonium acetate was determined to be 57°C. The rise in  $T_g$  can be expressed in terms of conversion (or extent of cure) according to eq. 3 (Fig. 16). Using the relationship between extent of conversion and time at different

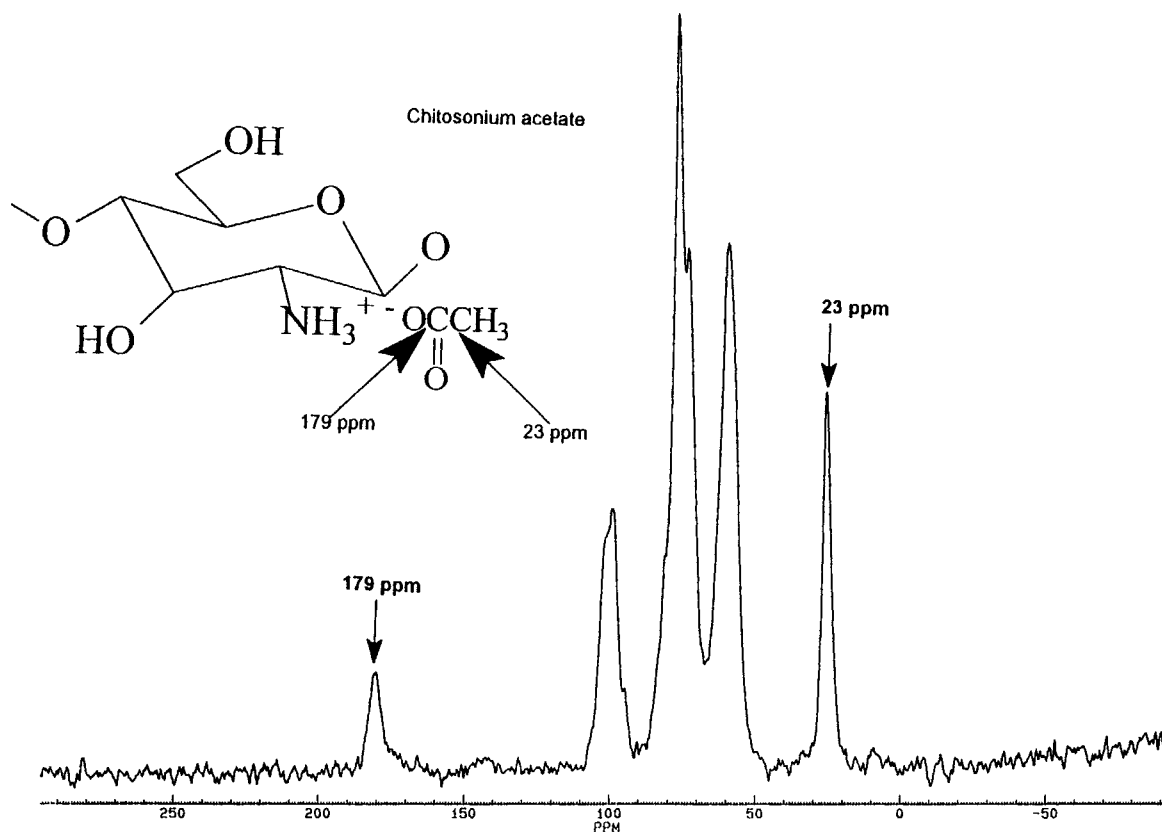


**Figure 11** CP-MAS  $^{13}\text{C}$ -NMR spectrum of chitosonium acetate. The peaks at 23 and 179 ppm are identifiable as methyl ( $\text{CH}_3$ ) and ionic *N*-acetate carbonyl groups, respectively.

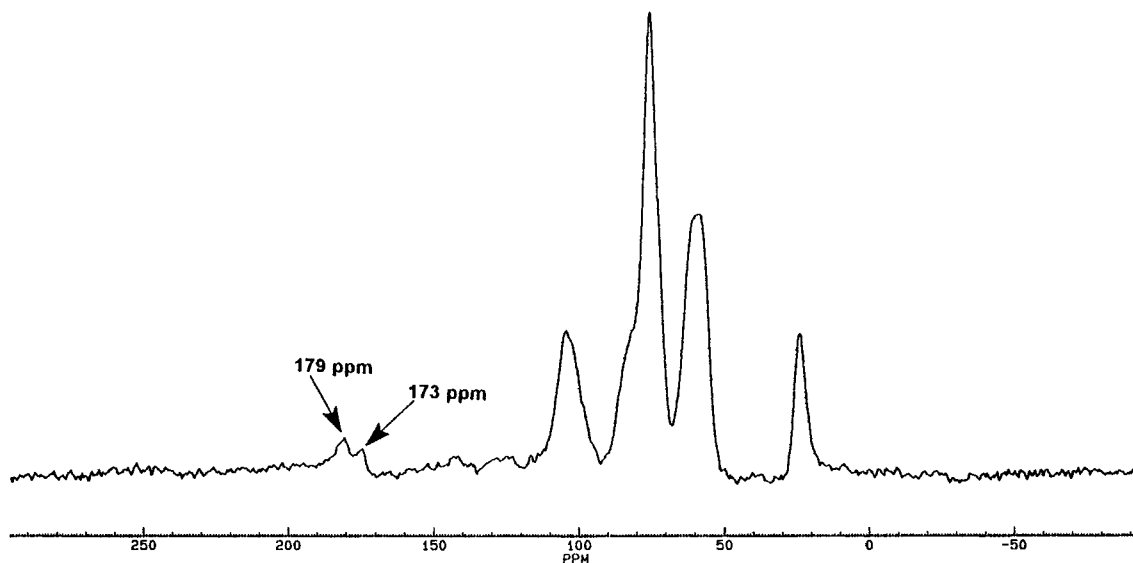


**Figure 12** CP-MAS  $^{13}\text{C}$ -NMR spectrum of chitosonium acetate that is subjected to heat treatment at  $100^\circ\text{C}$  for 12 h. Both the *N*-acetate and *N*-acetyl carbonyls are discernible.



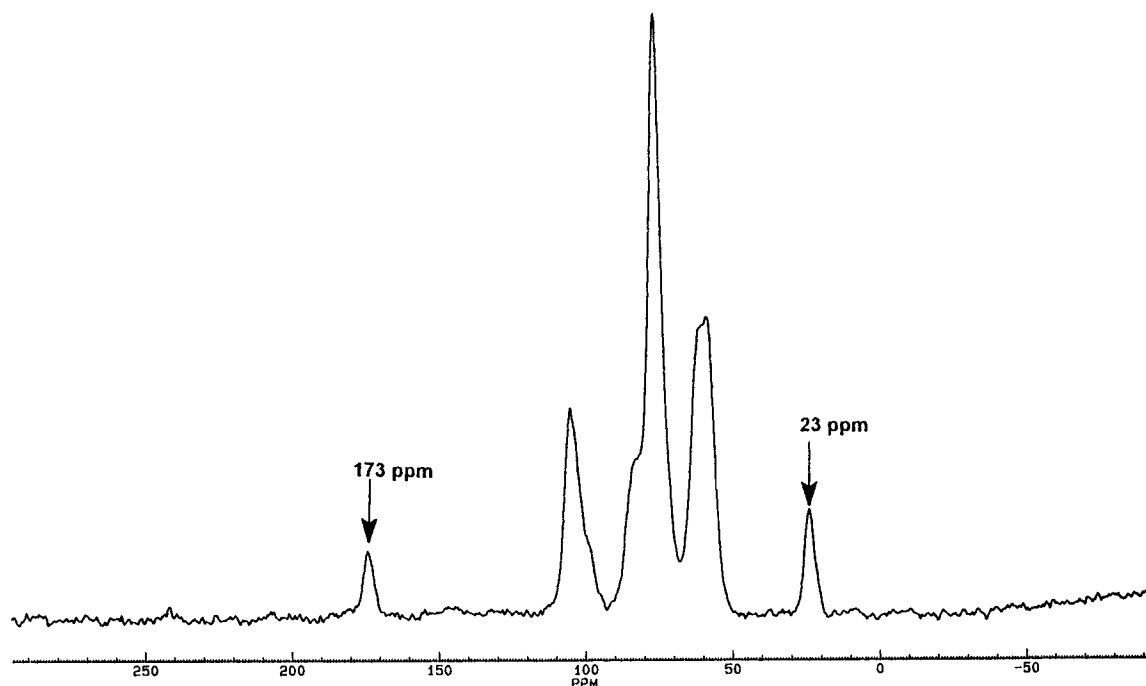


**Figure 13** CP-MAS  $^{13}\text{C}$ -NMR spectrum of chitosonium acetate that is subjected to heat treatment at  $100^\circ\text{C}$  for 12 h, followed by treatment with cold alkali. The *N*-acetate carbonyl at 179 ppm disappears as a result of this treatment, only leaving the *N*-acetyl carbonyl at 173 ppm.

isothermal cure temperature [eq. (2)], results emerge (Fig. 17) that indicate two sequential cure reactions both of which follow first-order kinetics. The initial, fast reaction has an activation energy of  $15 \text{ kcal mol}^{-1}$  and the second, late reaction reveals an activation energy of  $21 \text{ kcal mol}^{-1}$  (Fig. 18).

These results suggest that chitosonium acetate is capable of undergoing a transformation to chitin by heating, an amidization process, and that the process involves two sequential first-order reactions. This pattern of amidization is similar to the reported heat-induced transformation of polyamic acid to polyimide, an imidization process in which imidization proceeds by an initial fast reaction, followed by a substantially slower reaction.<sup>17,18</sup> In contrast to the amidization process, however, the activation energies of the imidization reaction were reported to be insignificantly different, i.e.,  $26 \pm 3 \text{ kcal/mol}$  and  $23 \pm 7 \text{ kcal/mol}$  for the initial, fast, and later, slow reactions, respectively.<sup>18</sup> The higher activation energies for the imidization process over amidization may be related to higher energy barriers associated with the ring closure that occurs in imidization with the loss of water. In the imidization process, the  $T_g$  of the material continually rises as conversion proceeds. Molecular motion is frozen in or restricted when the rising  $T_g$  becomes equal to and/or well

above the imidization temperature such that attainment of suitable conformation necessary for imidization is not possible. However, when the imidization temperature is raised to a value above the ultimate  $T_g$  of a corresponding fully cured (and, therefore, fully imidized) material, further imidization is possible. Therefore, it has been suggested that the existence of two sequential cure reactions could be related to restrictions on chain mobility. It would be expected, contrarily to the activation energies reported for the imidization process, that the slow, late reaction should be associated with a higher energy barrier, i.e., activation energy. This is because it would require a much higher activation energy to rearrange the polymer chains that are supposedly frozen in position to suitable conformations necessary for imidization to occur. This expectation is consistent with the activation energies of amidization reported in this study, i.e., a lower activation energy for the fast, initial reaction compared to the slow, late activation energy. Other studies suggest that the cure of amine-cured epoxy is considerably retarded once vitrification is reached, i.e., when the rising  $T_g$  becomes equal to the cure temperature. This is attributed to restrictions on chain diffusion necessary for the cure reaction to proceed.<sup>19</sup> Thus, it is reasonable to postulate that the existence of

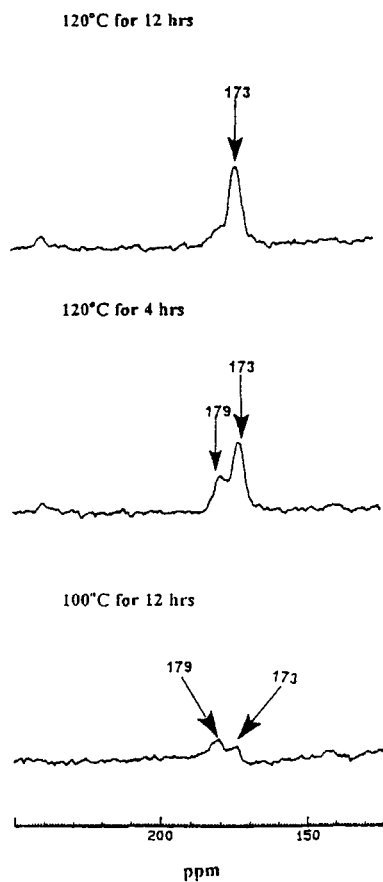


**Figure 14** CP-MAS  $^{13}\text{C}$ -NMR spectra of chitosonium acetate that is subjected to different severity of heat treatment. There is a progressive disappearance of the *N*-acetate carbonyl peak at 179 ppm with increasing severity of heat treatment.

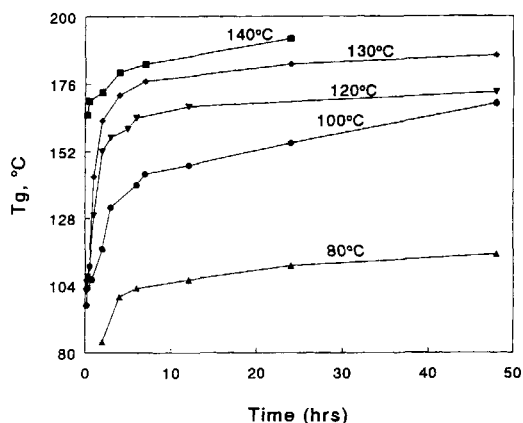


**Figure 15** Glass transition temperature variation with time at various isothermal cure temperatures. This figure is transformed, according to eq. 3, to conversion variation with time. The initial  $T_{g,0}$ , and maximum glass transition temperatures,  $T_{g,\infty}$ , were determined as 57 and 189°C, respectively.

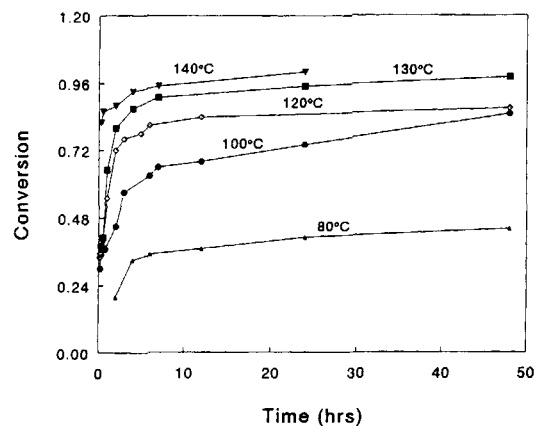


**Figure 16** Conversion, calculated using eq. 3, with time at various isothermal temperatures.

two sequential reactions involved in chitosonium acetate to chitin transformation has to do with limitations on chain mobility. Further studies to substantiate this postulate are being undertaken.

## CONCLUSIONS

1. Chitosonium acetate spontaneously converts to chitin at elevated temperatures. Thus, chitin is regenerated from a chitosan-acetic acid complex.
2. Chitosonium acetate to chitin transformations give rise to modulus and  $T_g$ -changes, which can be likened to the behavior of thermosets.

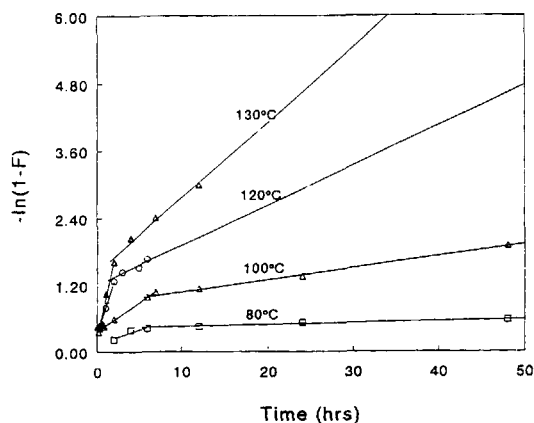


**Figure 17** First-order plot of chitosonium acetate to chitin transformation according to eq. 2. There is a change in slope of each line after prolonged heat treatment. This trend suggests that two sequential steps are involved in the chitosonium acetate to chitin transformation.

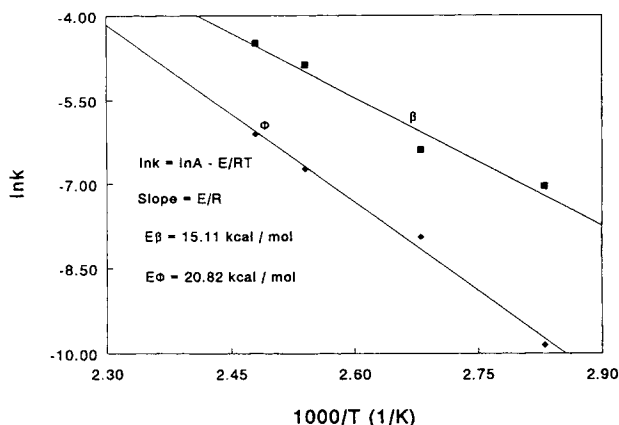


**Figure 18** Arrhenius plot of rate constants vs. temperature for activation energy determination of the amidization reaction involved in the transformation of chitosonium acetate to chitin. The activation energy is determined from the slope of the line according to eq. 4.  $\beta$ : First step reaction,  $\Phi$  second step reaction.  $E\beta$  and  $E\Phi$  are the corresponding activation energies.

3.  $T_g$ -changes can be used to describe the kinetics of chitosonium acetate-to-chitin transformations.
4. Two first-order rate equations, which adequately describe the chitosonium acetate-to-chitin transformation, suggest two distinct reaction phases: an initial phase with an activation energy of 15 kcal mol<sup>-1</sup>, and a late phase with an activation energy of 21 kcal mol<sup>-1</sup>.
5. The transformed material behaves in several respects like a thermoset, especially in terms of  $T_g$  and modulus rise with time, and tan  $\delta$ -decline.

This is to thank Mr. Jianwen Ni, Department of Wood Science and Forest Products, Virginia Tech, for his assistance with the solid state NMR spectroscopy.

## REFERENCES

1. R. A. A. Muzzarelli, in *Encyclopedia of Polymer Science and Engineering*, Vol. 3, Wiley, New York, 1985, pp. 430-440.
2. L. L. Balassa and J. F. Prudden, in *Proceedings of the First International Conference on Chitin and Chitosan*, R. A. A. Muzzarelli and E. R. Pariser, Eds., MIT, Cambridge, MA, 1978.
3. P. L. Sapelli, in *Chitin in Nature and Technology*, R. A. A. Muzzarelli, Ed., Plenum Press, New York, 1986.
4. M. Nakajima, K. Atsumi, K. Miura, and H. Kanamaru, *Jpn. J. Surg.* **16**, 418 (1986).
5. F. A. Rutherford and P. R. Austin, in *Proceedings of the First International Conference on Chitin and Chitosan*, R. A. A. Muzzarelli and E. R. Pariser, Eds., MIT, Cambridge, MA, 1978.
6. B. L. Averbach, in *Proceedings of the First International Conference on Chitin and Chitosan*, R. A. A. Muzzarelli and E. R. Pariser, Eds., MIT, Cambridge, MA, 1978.
7. H. R. Hepturn and H. D. Chandler, in *Proceedings of the First International Conference on Chitin and Chitosan*, R. A. A. Muzzarelli and E. R. Pariser, Eds., MIT, Cambridge, MA, 1978.
8. S. Mima, M. Miya, R. Iwamoto, and S. Yoshikawa, *J. Appl. Polym. Sci.*, **28**, 1909-1917 (1983).
9. G. E. East and Y. Qin, *J. Appl. Polym. Sci.*, **50**, 1773-1779 (1993).
10. Y. C. Wei, S. M. Hudson, J. M. Mayer, and D. L. Kaplan, *J. Polym. Sci., Part A*, **30**, 2187-2193 (1992).
11. J. Hosokawa, M. Nishiyama, K. Yoshihara, and T. Kubo, *Ind. Eng. Chem. Res.*, **29**, 800-805 (1990).
12. A. Isogai and R. H. Atalla, *Carbohydr. Polym.*, **19**, 25-28 (1992).
13. J. K. Gillham, in *Structural Adhesives*, A. J. Kinloch, Ed., Elsevier Applied Sci. Pub., New York, 1986.
14. K. Hofmann and W. G. Glasser, *Thermochim. Acta*, **166**, 169-184 (1990).
15. M. Pizzoli, G. Ceccorulli, and M. Scandola, *Carbohydr. Res.*, **222**, 205-213 (1991).
16. T. Provder, R. M. Holsworth, and T. H. Grentzer, in *Adv. Chem. Ser. 203*, American Chemical Society, Washington, D. C., 1981.
17. S. Numata, K. Fujisaki, and N. Kinjo, in *Polyimides: Synthesis, Characterization and Applications*, Vol. 1, K. L. Mittal, Ed., Plenum, New York, 1984.
18. J. A. Kreuz, A. L. Endrey, F. P. Gay, and C. E. Sroog, *J. Polym. Sci., Part A1*, **4**, 2607-2616 (1966).
19. G. Wisanrakkit and J. K. Gillham, *J. Appl. Polym. Sci.*, **41**, 2885-2929 (1990).

Received July 17, 1995

Accepted November 1, 1995